Expected annual loss oriented seismic retrofitting optimization of RC framestructures using a new AI-based framework

COMPDYN 2021
8th ECCOMAS Thematic Conference on
Computational Methods in Structural Dynamics and Earthquake Engineering
M. Papadrakakis, M. Fragiadakis (eds.)
Streamed from Athens, Greece, 27–30 June 2021

EXPECTED ANNUAL LOSS ORIENTED SEISMIC RETROFITTING OPTIMIZATION OF RC FRAMESTRUCTURES USING A NEW AI-BASED FRAMEWORK

Fabio Di Trapani[1], **Antonio Pio Sberna**[1] **and Giuseppe Carlo Marano**[1]

[1] *Politecnico di Torino. Dipartimento di Ingegneria Strutturale, Edile e Geotecnica*
Corso Duca degli Abruzzi 24, 10129, Turin, Italy
e-mail: {fabio.ditrapani, antonio.sberna, giuseppe.marano}@polito.it

Abstract

The paper proposes a new genetic algorithm-based framework aimed at efficiently design multiple seismic retrofitting interventions for reinforced concrete (RC) frame structures minimizing the costs of intervention. The feasibility of each tentative solution is assessed by considering in indirect way the expected annual loss (EAL). EAL evaluation is performed referring to different limit states whose repairing costs are expressed as a percentage of reconstruction costs and evaluating the respective mean annual frequency of exceedance. To effectively engage both serviceability and ultimate limit states, the compresence of two different retrofitting systems is considered. Steel bracings are used to increase the global stiffness of the structure and improve operational and damage limit states performance. FRP wrapping of columns is used to manage the life safety and collapse limit state demands. The optimization carried out by the novel AI-based framework implementing a genetic algorithm (GA). For both the retrofitting systems, their position within the structure (topological optimization) and their sizing are provided as output. Results will show that seismic retrofitting can be effectively optimized to minimize costs controlling the expected annual loss.

Keywords: structural optimization, genetic algorithm, seismic retrofitting, expected annual loss, FRP, bracing

1 INTRODUCTION

The pressing necessity of reducing the seismic vulnerability of existing structures located in earthquake-prone regions has motivated the last decade of research activities to address the seismic retrofitting techniques. Despite the large availability of retrofitting solutions with different materials and arrangement techniques, nowadays, there are no formal methods for designing this kind of interventions simultaneously controlling the resulting overall seismic performance. Therefore, in most cases, the choice of retrofitting position and amount are

exclusively entrusted to the experience and intuition of the designer. A first consequence of this empirical approach is that several trial-and-error attempts are required to find a feasible retrofitting solution. This also requires considerable time consumption to get a sufficient compromise between safety and costs. Secondly, results so obtained are not controlled in cost or in performance, therefore, obtained retrofitting solutions are feasible do not ensure maximum exploitation or the retrofitting with a consequent increase of intervention costs, invasiveness, and downtime.

In the last years, the scientific interest in structural optimization was mainly focused on sizing and shape optimization of new structures. On the contrary, the optimization of seismic retrofitting of existing structures has not been investigated many times, while noticeable interest is emerging in the last years. Few researchers have addressed the problem of the optimization of FRP jackets (Chisari and Bedon 2016 [1], Seo et al. 2018 [2]) or other applications of seismic retrofitting devices for RC buildings by using fluid viscous dampers (Pollini et al. 2017 [3]), dissipative bracings (Braga et al. 2019 [4]) or both (Lavan and Dargush 2009 [5]). More recent studies addressed the issue of optimization of seismic retrofitting costs. Among these, Falcone et al. 2019 [6] proposed a framework for optimizing the realization costs of FRP jacketing and steel bracings for existing RC frame structures through genetic algorithm optimization. Papavasileiou et al. 2020 [7] faced retrofitting optimization of encased steel-concrete composite columns comparing three different retrofitting methods: concrete jacketing, steel jacketing and steel bracing. A similar approach was followed by Di Trapani et al. 2020 [8] who proposed an innovative framework based on genetic algorithm aimed at minimizing steel jacketing seismic retrofitting costs for ductility deficient RC structures. These very recent research activities addressed their efforts in defining new effective algorithms focused on the optimization of the retrofitting interventions to minimize their cost. This provided an answer to the issue raised above, that is getting the control of the design to achieve an output goal. A more generalized view of this problem is faced in this paper, whose purpose is the development of a new optimization framework aimed at optimizing service-life costs of structures subject to retrofitting interventions, whit special regard to RC frame structures. The expected annual loss (EAL) has been proved as valid tool to compare structure seismic performance during their service life Calvi (2013) [9]. It estimates the overall behaviour of the construction in terms of expected economic annual losses associated with seismic events that could take place during the reference service life.

The goal of the proposed framework is to determine, for a non-seismically conforming RC building, the best retrofitting configuration in terms of position (topological optimization) and amount of reinforcement (sizing optimization). Optimization focuses on the minimization of retrofitting costs considering in an indirect way the resulting EAL value.

Since EAL assessment involves different limit states satisfaction, the proposed framework considers multiple retrofitting interventions. In particular, the case study of a 3D multistorey RC building is considered supposing FRP jacketing of RC columns (to increase ductility) and steel bracings (to reduce lateral deformability) as retrofitting interventions to optimize.

The optimization process is carried out by a genetic algorithm (GA) developed in MatLab®. The structural performance of each solution is assessed from the results of static pushover analyses in the framework of the N2 method. The validity and efficiency of the proposed method is proved by implementing it on a case study structure. Eventually, the results are compared with the outcomes of a cost optimization that does not consider EAL control. The presented methodology is still under development, but it constitutes a novel contribution towards the use of artificial intelligence techniques to improve design effectiveness and sustainability.

2 OPTIMIZATION FRAMEWORK

The optimization framework herein proposed is based on a genetic algorithm (GA) optimization routine developed in MatLab®. The optimization algorithm relates a structural model developed with the *OpenSees* software platform (McKenna et al. 2000 [10]) with the GA process. The genetic algorithm is an evolutionary algorithm inspired by the evolution theory, therefore, is generates a *population* of *individuals* representing different tentative retrofitting arrangements. Each individual handled by algorithm is characterized by a *design vector* collecting all the decision variable to be optimized. Each design vector is associated with a potential retrofitting configuration. The optimization involves the definition of a proper *objective function*, taking into account both the feasibility of a solution (namely the passing safety checks) and cost associated to the retrofitting intervention. A schematic flowchart of the proposed framework is depicted in Fig. 1, which structure is discussed in detail in the following sections.

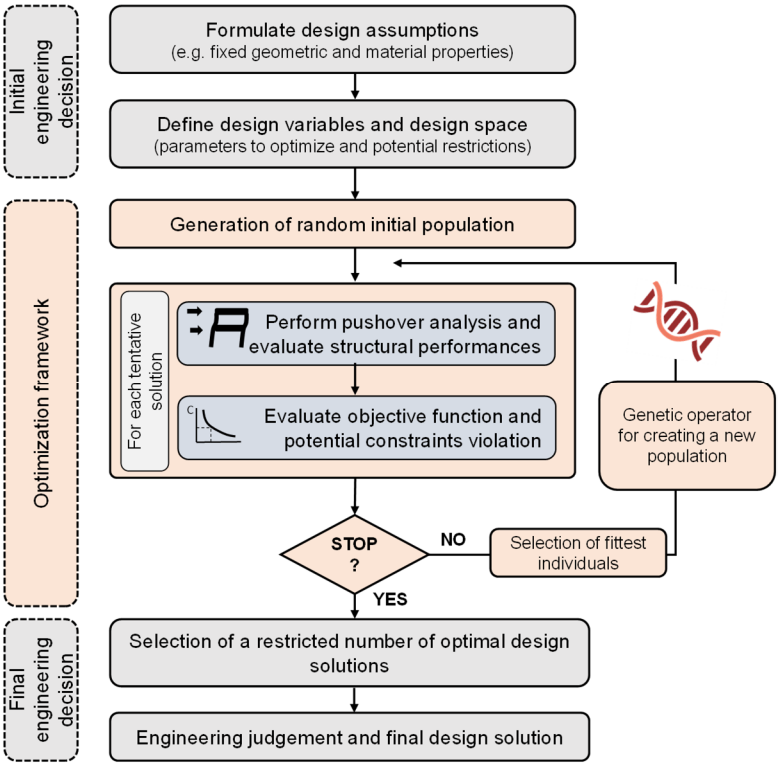

Figure 1: Flowchart of the optimization framework.

2.1 Definition of the EAL

The expected annual loss represents percentage annual loss of economic value of a structure in its reference life taking into account the associated seismic risk, which basically depends on the site hazard and on the structure seismic vulnerability. The determination of the EAL requires therefore the assessment of the performance of the structure to different limit states, associated with the respective return periods $T_{r,LS}$ and annual rates of failure, expressed as the inverse of the return periods ($\lambda_{LS} = 1/T_{r,LS}$). The achievement of a limit state is associated with a specific repair cost. The EAL curve connects the annual rate of failure of each limit state with the respective repairing cost. A simplified method to compute EAL has been proposed by Cosenza et al. (2018) [11]. According to this approach repair costs are expressed as percentages of the

repair costs (%RC) with respect to the reconstruction cost (reconstruction limit state (RLS)) and are fixed for each limit state (Fig. 2a).

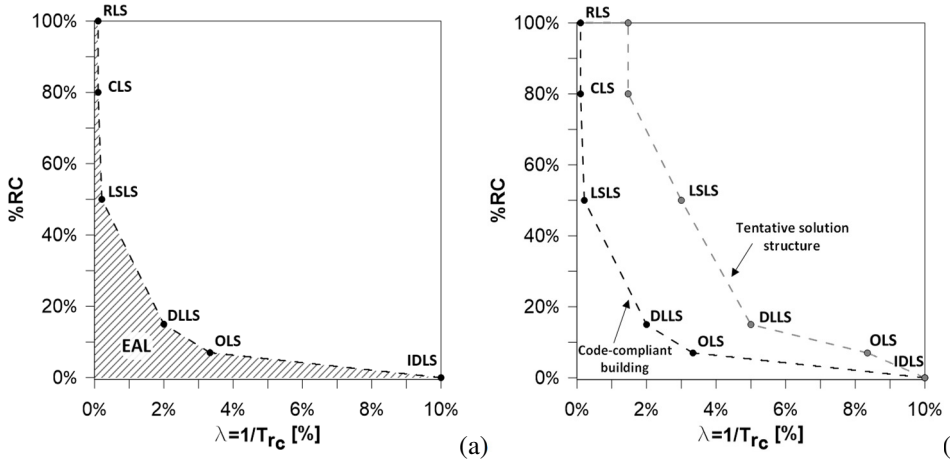

Figure 2: Expected Annual Loss curve: (a) formal EAL determination; (b) code compliant building EAL curve and generic EAL curve for a building.

According to Cosenza et al. (2018) [11], eight limit states are identified by reconstruction limit state (RLS) and collapse limit state (CLS) which are associated with repair cost (%RC) equal to 100% and 80%, respectively. Moreover, the %RC for the life safety limit state (LSLS) is set to 50%. Service limit states are the damage limitation limit state (DLLS) and the operational limit state (OLS). These two former limit states have a %RC of 15% and 7% respectively. The initial damage limit state (IDLS) is characterized by repair costs equal to zero and a mean annual frequency of exceedance that is conventionally assumed as $\lambda_{IDLS} = 10\%$. For a code-compliant structure, namely a structure having for each limit state a capacity that is exactly equivalent to the demand, the annual rates of exceedance of each limit states for the associated (fixed) reconstruction costs and are those reported in Table 1. Considering values in Table 1, the EAL of the code compliant building is 1.13%.

Limit state	**%RC**	$T_{r,LS}$ [years]	$\lambda_{LS}=1/T_{r,LS}$ [%]	EAL_{cc}
RLS	100	∞	0.00	1.13%
CLS	80	975	0.10	
LSLS	50	475	0.21	
DLLS	15	50	2.00	
OLS	7	30	3.33	
IDLS	0	10	10.0	

Table 1: Mean annual frequency of exceedance (λ) and repair costs (%RC) associated with each LS for a code-compliant building.

Formally the EAL is evaluated as the area under the curve that connect the points (λ, %RC) for each limit state (Fig. 1a), so that:

$$EAL = \sum_{1=2}^{5} \left[\lambda_{LS(i-1)} = \lambda_{LS(i)} \right] \cdot \left[\%RC_{LS(i)} = \%RC_{LS(i-1)} \right] / 2 + \lambda_{CLS} \cdot \%RC_{RLS} \quad (1)$$

For the code-compliant building Eq. 1 results in EAL=1.13%. The evaluation of the EAL for a generic structure can be carried out performing a pushover results to determine return period associated with occurrence of each limit state ($T_{rC,LS}$). A simplified expression [11], based on the determination of the safety factor ($\zeta_{E,LS}$) can be used to evaluate capacity return period for each limit state as follows:

$$T_{rC,LS} = T_{rD,LS} \cdot \left(\zeta_{E,\mathrm{LS}}\right)^{\eta} \tag{2}$$

where the parameter η can be approximated to $\eta = 1/0.41$ and the safety factors can be calculated for the damage limitation limit state (DLLS) and life safety limit state (LSLS) as:

$$\begin{cases} \zeta_{E,LSLS} = \dfrac{PGA_{c,LSLS}}{PGA_{d,LSLS}} \\ \zeta_{E,DLLS} = \dfrac{d^{*}_{max,DLLS}}{S_{de,\mathrm{DLLS}}\left(T^{\star}\right)} \end{cases} \tag{3}$$

where $PGA_{d,\mathrm{LSLS}}$ is the peak ground acceleration demand and $PGA_{c,\mathrm{LSLS}}$ is the peak ground acceleration capacity, that is the one associated with the earthquake inducing LS limit state. The latter can be evaluated from the results of a pushover analysis in the framework of the N2 method (Fajfar 2000 [12]). In Eq. 3, $S_{de,\mathrm{DLLS}}\left(T^{\star}\right)$ is the displacement demand associated with elastic DLLS spectrum, and $d^{*}_{max,\mathrm{DLLS}}$ is the top displacement associated with the achievement of the DLLS condition. This can be assessed by evaluating the maximum interstory drift. For instance, the value of $d^{*}_{max,\mathrm{DLLS}}$ can been evaluated as the top displacement of the structure at which the larger interstory drift exceeds a limit drift $\delta_{i,\max}$.

The corresponding annual rates of failure are then obtained as $\lambda_{LS} = 1/T_{rC,LS}$. According to **[11]**, the annual rates of failure for the operational and collapse limit states are obtained as a function of those evaluated for DL and LS limit state, so that:

$$\begin{cases} \lambda_{OLS} = 1.67 \cdot \lambda_{DLLS} \\ \lambda_{CLS} = 0.49 \cdot \lambda_{LSLS} \end{cases} \tag{4}$$

Therefore, EAL is known once obtained λ_{DLLS} and λ_{LSLS}.

2.2 Definition of the design vector

The framework aims at optimizing the intervention cost of two different retrofitting systems: FRP wrappings of columns and concentric steel bracings. The decision variables that encode the position and sizing of both retrofit are collected together into a so-called design vector. With reference to Fig. 3, the selected design variables are the number of braced frame fields (n_{br}), the diameter of braces (ϕ_{br}), the number of layers of FRP (n_{FRP}), and the position of the columns retrofitted by the FRP. Design variables are gathered in the design vector **b** so defined:

$$\mathbf{b} = \begin{pmatrix} n_{br} & \phi_{br} & n_{FRP} & \mathbf{p} \end{pmatrix}^{T} \tag{5}$$

in which the term **p** is an array of binary numbers representing the position of the FRP retrofitted columns defined as:

$$\mathbf{p} = \begin{bmatrix} \dots & \dots & c_{ij} & \dots \end{bmatrix}^{\mathrm{T}} \tag{6}$$

in which the generic element c_{ij}, is a Boolean number assuming the value 1 if a column is retrofitted and 0 if not. The subscript *i* indicates the position of a column in plan and *j* the storey. The term n_{FRP}, instead, is a natural value that represents the number of overlapping layers of FRP on each column belonging to the interval:

$$n_{\text{FRP}} \in \left[1, n_{\text{FRP,max}}\right] \tag{7}$$

where $n_{FRP,max}$ is the maximum number of FRP layers allowed.

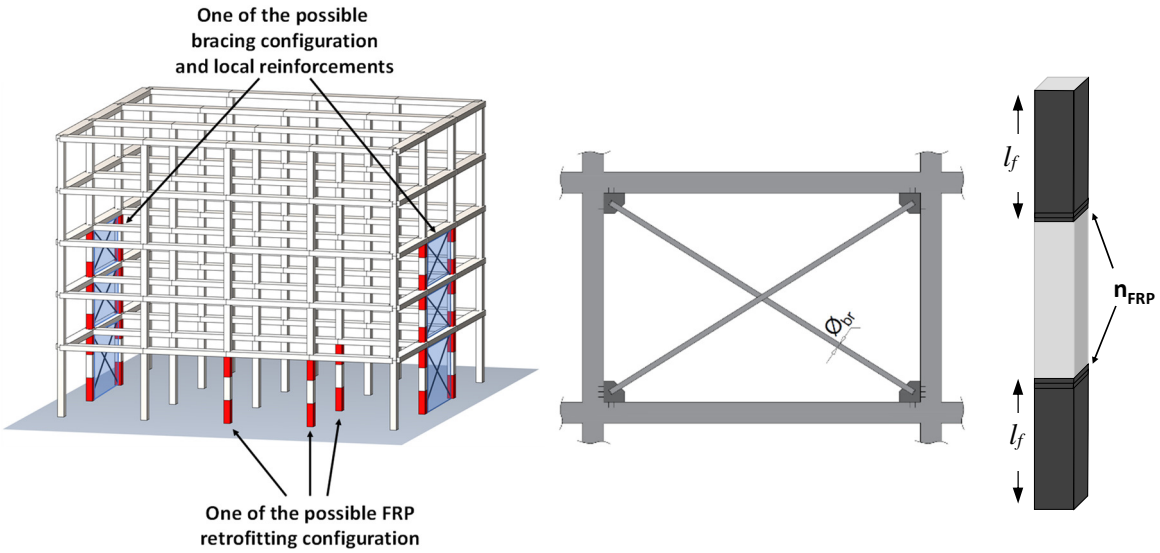

(a) (b) (c)

Figure 3: Representation of the design variables: (a) Generic FRP and bracing retrofitting configuration for a RC frame structure; (b) Usual circular steel bracings installation with generic diameter ($Ø_{br}$); (c) Typical FRP arrangement for ductility reasons with a generic number of fabric layers (n_{FRP}).

To prevent premature collapse of columns that are adjoining to the bracing systems due to the additional shear demand, it is provided that they are reinforced with at least one layer of FRP. To introduce this local reinforcement into the design vector (if not already present in the retrofitting configuration) a heuristic repair technique is employed. By controlling the position of the bracings, the algorithm adjusts the vector $\mathbf{p}$ so that the columns adjacent to the bracings are reinforced with FRP.

To reduce the computational effort, the following simplifying hypotheses are introduced for the retrofitting system:

i) FRP fabrics have fixed height (h_f) and thickness ($t_{f,1}$).
ii) Confinement of columns is realised by applying the FRP for a length (l_f) at both terminal part of the column where the maximum ductility demand is expected.
iii) The number of FRP layers is constant for all the retrofitted columns.
iv) Bracings are realised with circular cross-section steel elements. Their characteristics are constant for every frame.

2.3 Definition of the objective function

The objective function is aimed at the minimization the retrofitting intervention considering the realization of the two retrofitting systems as:

$$F = C_{\text{br}} + C_{\text{FRP}} \tag{8}$$

where C_{br} is the cost related to the arrangement of bracings and C_{FRP} is the one for the realization of the FRP wrapping of the columns. Both terms consider the material and manpower costs and the necessary works for the demolition and restoration of adjoining plaster and masonry. The first one can be evaluated as:

$$C_{\mathrm{br}} = \sum_{i=1}^{n_{br}} \left(W_{\mathrm{br},i} \cdot c_{\mathrm{br}} \right) + n_{\mathrm{br}} \cdot c_{\mathrm{br,m}} \tag{9}$$

where c_{br} is the manpower and material cost per unit weight (estimated in $c_{\mathrm{br}} = 6$ €/kg), $c_{\mathrm{br,m}}$ is the fixed cost related to the demolition and reconstruction of masonry (2000€ every braced frame fields), and $W_{\mathrm{br,i}}$ is the weight of the bracings in the i-th frame field that can be evaluated as:

$$W_{\mathrm{br}} = 2 \cdot L_{\mathrm{br}} \cdot \left(\frac{\phi_{\mathrm{br}}}{2} \right)^2 \cdot \pi \cdot \gamma_s \tag{10}$$

in which L_{br} is the length of one bracing and γ_s is the specific weight of the steel ($78.5\ \mathrm{kN/m^3}$).

As regards FRP retrofitting the cost is computed as follows: C_{FRP} is computed as:

$$C_{\mathrm{FRP}} = \sum_{i=1}^{n_c} \left(A_{\mathrm{FRP,i}} \cdot c_{\mathrm{FRP}} \right) + n_c \cdot c_{\mathrm{FRP,m}} \tag{11}$$

where n_c is the number of retrofitted columns taking into account also the local reinforcement of the columns adjoining the steel bracings systems as presented in the previous section, c_{FRP} is the unit cost of the FRP (estimated in $c_{\mathrm{FRP}} = 300\,€/\mathrm{m^2}$), $c_{\mathrm{FRP,m}}$ is the cost per column for the demolition and reconstruction of adjacent masonries and plasters and A_{FRP} is the area of the FRP fabric used to retrofit the generic column. The latter can be computed starting from the geometric dimensions of each column cross-section (b and h); supposing that the edges of the columns are rounded with a r_c radius, and the fabrics are applied for a length l_f at both end of the columns:

$$A_{\mathrm{FRP}} = \left[2 \cdot (b+h) - (4-\pi) \cdot r_c^2 \right] \cdot 2 l_f \tag{12}$$

As presented in the previous section, the EAL assessment is ruled only by the evaluation of λ_{DLLS} and λ_{LSLS}, thus the feasibility of each solution is restrained by the simultaneous verification that:

$$\lambda_{t_{\mathrm{DLLS}}} \le \lambda_{ccb_{\mathrm{DLLS}}} \quad \& \quad \lambda_{t_{\mathrm{LSLS}}} \le \lambda_{ccb_{\mathrm{LSLS}}} \tag{13}$$

which implies:

$$EAL \le EAL_{cc} \tag{14}$$

A non-penalty approach is developed to take into account the feasibility (or not) of each tentative solution as explained in the following section.

2.4 Optimization algorithm subroutines

The search for the optimal solution through the use of GA algorithms proceeds generating a first population by randomly creating a series of individuals encoded by design vectors as

presented in the previous section. Analysing each of the population's tentative solutions, the value of fitness and the number of violated constraints is estimated.

Two different genetic operators are employed to improve the genes of the individuals at the end of each generation, the crossover, which mixes the genomes of the best individuals and the mutation, preventing local optima stuck by introducing random slight changes. The framework proceeds until one of the stopping criteria is achieved. For the current cases, only two stopping criteria on maximum number of generations and stall are imposed. In the ensuing Figure 4 a schematic flowchart of the subroutines is depicted.

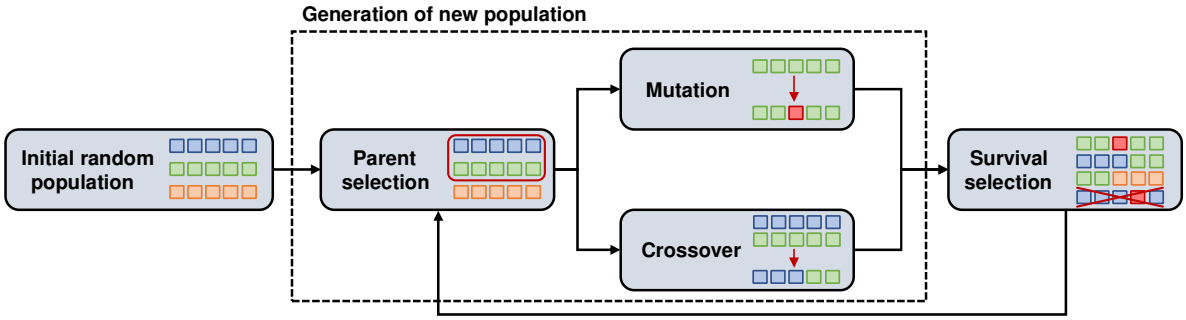

Figure 4: Schematic flowchart of the genetic algorithm process.

2.4.1. Parent selection

Parent selection is the subroutine entrusted with selecting individuals that have to be handled by other genetic operators (mutation and crossover). For the current application, random tournament selection is employed. It is based on a direct comparison of individual's performance. Within the individuals of the generation, k individuals are randomly selected (where k is called *tournament size*), among them the best individual is chosen as parent for the ensuing mating process. The comparison is carried out firstly by checking the number of violated constraints and then with respect to the fitness value. In this way, individuals with the lowest number of constraints violated are preferred. If the individuals have the same number of constraint violations the individual with the best fitness is chosen.

2.4.2. Crossover and mutation

Crossover and mutation operators are employed to improve the chromosomes at each generation. While the former works by mixing chromosomes selected by the parent selection, the latter is the genetic operator who is mainly entrusted with introducing the random component in creating offspring.

A single point mutation function is employed in the proposed GA framework. It works by selecting one random position along the design vector and changing the value of that design variable. For Boolean variables included in the $\mathbf{p}$ sub-vector (Eq. 10) the mutation of a gene is simply a switch from 0 to 1 or vice-versa. In case the mutation ha

s to be achieved on the discrete values of the design vector, a new random number among the possible ones is chosen.

For the crossover subroutine, a new specific procedure has been defined to correctly handle heterogeneous genomes such as those of the proposed framework. For the binary string $\mathbf{p}$, a single point crossover is employed (Fig. 5). The operating principle provides the random selection of a locus along the string called crossover point. The child individual is constructed by

picking from the beginning of the chromosome to the crossover point from one parent; the rest is copied from the second one.

The crossover of the natural decision variables is conducted by randomly choosing a new value among the corresponding values of the parents. This new crossover function, which can be called *random intermediate value crossover*, is implemented to smoothly mix the parents chromosomes. An example of the proposed crossover procedure is depicted in Fig. 5.

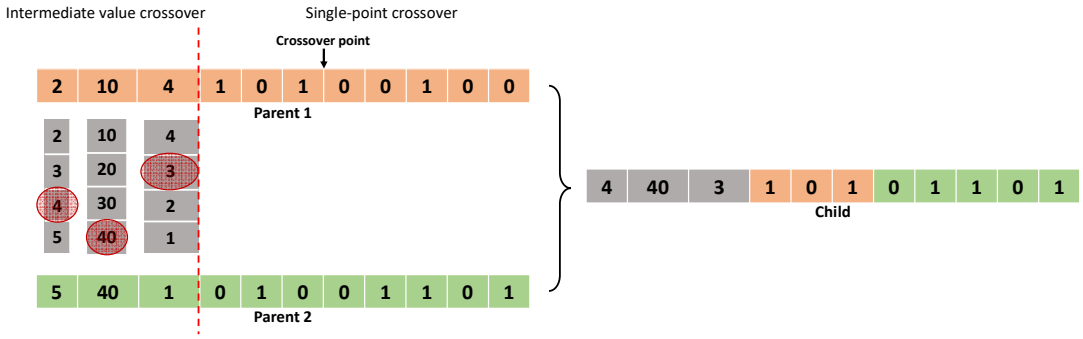

Figure 5: Example of the proposed crossover procedure.

2.4.3. Survival selection

The selection of the best individuals at the end of each generation is a fundamental step for optimization process success. The function entrusted with this task has to reject the individuals with low fitness to allow the best individuals to spread their genome. Moreover, as defined in Eq.5, the fitness evaluation does not consider the feasibility of tentative solutions; hence the selection function is responsible for managing the two constraints (Eq. 7).

A new survival selection function is developed to handle both individual's fitness and feasibility constraints efficaciously. The operating principle provides a double sorting process, first ordering the individuals with respect to the number of violated constraints and then among the individuals with the same number of constraint violation for the fitness value.

Eventually, only the best individuals are taken for the next generation. This new function that can be called *sorting and truncation selection*¸ has proved a valid operator to manage constrained optimization problems without requiring penalty approaches.

3 REFERENCE STRUCTURAL MODEL

The proposed framework is interfaced with a FE software to execute structural analysis. For the current application the *OpenSees* software platform. Modelling assumptions are described in detail in this section.

3.1 Modelling of reinforced concrete elements with and without FRP and of steel braces

Frame elements are modelled adopting distributed plasticity force-based elements with five Gauss-Lobatto integration points present in OpenSees (Fig. 6).

Concrete elements are modelled using a *Concrete01* uniaxial material model for the cross-section fibers. In order to simulate the crushing of the cross-section fibers, Concrete01 material is combined with *MinMax* material, which removes the contribution of a fiber when a specified strain threshold is achieved. Steel rebars are modelled using the *Steel02* Giuffrè-Menegotto-Pinto material model (elasto-plastic with linear strain hardening).

The confined concrete model adopted for RC elements with and without retrofitting is the standard confined parabola-rectangle. According to the Italian Technical Code [13] and

Eurocode 8 [14] this model can be adopted for concrete elements confined by stirrups only or stirrups and FRP wrapping.

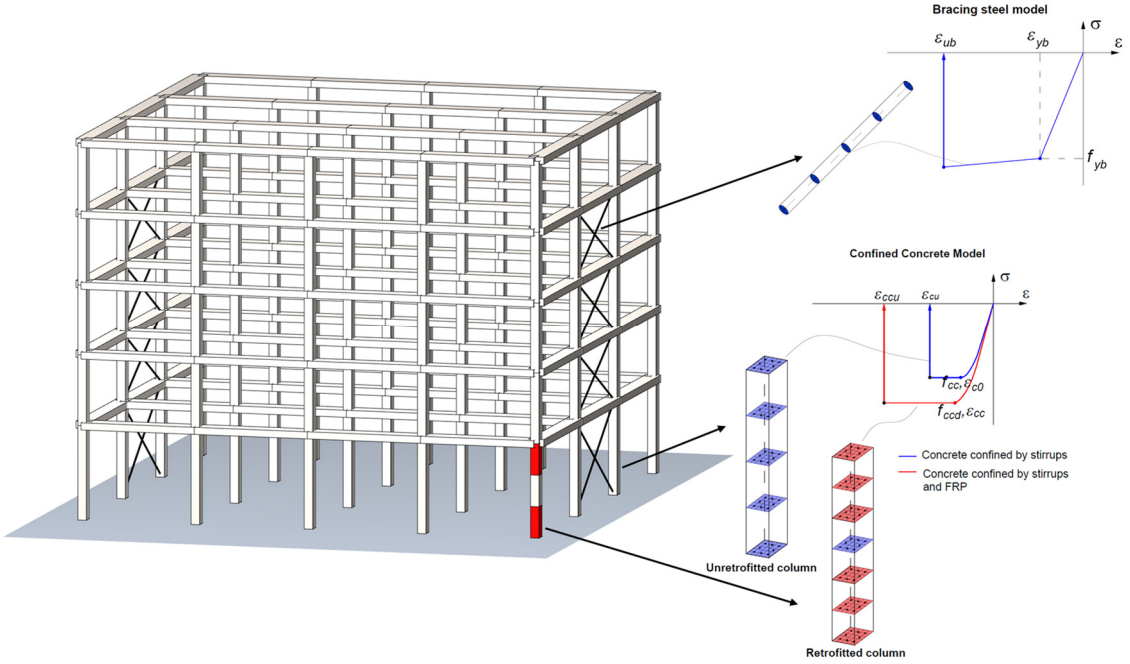

Figure 6: Definition of the fiber-section elements in OpenSees, concrete elements with and without FRP wrapping and steel bracings.

For the sake of brevity, the formulation of the model is here briefly recalled only for the RC elements wrapped by FRP. In detail, the confined peak stress is obtained as:

$$f_{\mathrm{ccd}} = f_{\mathrm{cd}} \cdot \left(1 + 2.6 \cdot \left(\frac{f_{\mathrm{l,eff}}}{f_{\mathrm{cd}}}\right)\right) \tag{15}$$

where f_{cd} is the peak stress of the concrete confined by stirrups and $f_{l,\mathrm{eff}}$ is the effective lateral confinement pressure that can be evaluated as:

$$f_{l,\mathrm{eff}} = k_{\mathrm{eff}} \cdot f_l \tag{16}$$

where f_l is the confinement pressure exerted by the FRP that can be calculated as:

$$f_l = \frac{1}{2} \cdot \rho_f \cdot E_f \cdot \varepsilon_{fd,\mathrm{red}} \tag{17}$$

in which E_f is the elastic modulus of the FRP (along the fiber direction), $\varepsilon_{fd,\mathrm{red}}$ is the reduced FRP peak strain that, in case of ductility evaluations, can be obtained as:

$$\varepsilon_{\mathrm{fd,red}} = \eta_a \cdot \frac{\varepsilon_{fk}}{\gamma_{\mathrm{f}}} \leq 0.6 \cdot \varepsilon_{fk} \tag{18}$$

where ε_{fk} is the design rupture strain of FRP reinforcement, η_a is the environmental reduction factor, and γ_{f} is the partial factor of FRP materials. In Eq. 15, ρ_f is the geometric reinforcement percentage that, in case of rectangular cross-section and continuous confinement (FRP is not applied in strips), can be calculated as:

$$\rho_f = \frac{2 \cdot t_f \cdot (b+h)}{(b+h)} \tag{19}$$

where b and h are the cross-section dimensions, and t_f is the thickness of FRP wrapping. The latter is calculated as the number of layers (n_{FRP}) encoded into the design vector (Eq. 5) that multiple the thickness of the FRP fabric ($t_f = n_{\text{FRP}} \cdot t_{f,1}$).

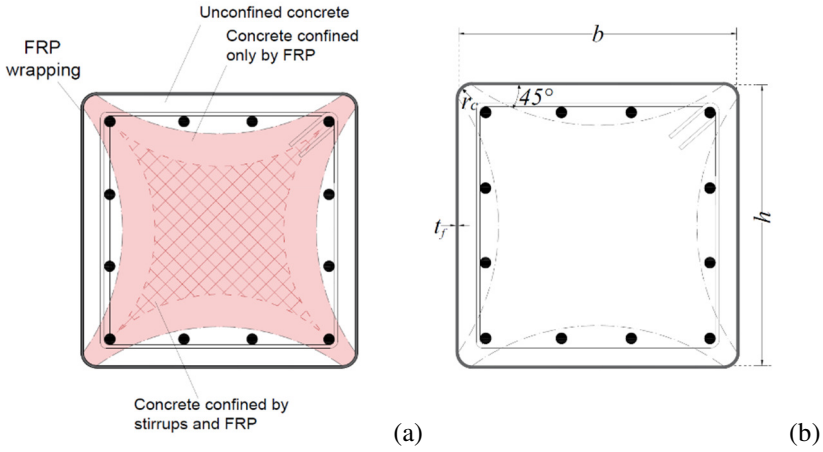

Figure 7: Configuration of the cross-section of columns retrofitted by FRP wrapping: (a) effectively confined area by stirrups and FRP; (b) geometric dimensions.

In Eq. 14 the coefficient k_{eff} represents the confining efficiency that can be calculated as the product of three different factors:

$$k_{\text{eff}} = k_v \cdot k_\alpha \cdot k_h \tag{20}$$

where k_v is the vertical confining efficiency, k_α is related to the fabric tilt, and k_h is the coefficient that represent the confining effect on the cross-section. They can be calculated in accordance with Eurocode [14], for a rectangular cross-section as:

$$k_v = \left(1 - \frac{p'_f}{2 \cdot min\{b;h\}}\right)^2; \quad k_\alpha = \frac{1}{1+\left(\tan\alpha_f\right)^2}; \quad k_h = 1 - \frac{(b-2r_c)^2 + (h-2r_c)^2}{3 \cdot b \cdot h} \tag{21}$$

In the previous equations p'_f is the distance between FRP strips, α_f is the tilt angle with respect the horizontal axis, r_c is the radius of the rounded corner.

The confined peak strain ε_{cc} and the confined ultimate strain ε_{ccu} can be evaluated as:

$$\varepsilon_{\text{cc}} = \varepsilon_{\text{c0}} \cdot \left(\frac{f_{\text{ccd}}}{f_{\text{cd}}}\right)^2; \quad \varepsilon_{\text{ccu}} = 0.0035 + 0.015 \cdot \sqrt{\frac{f_{\text{l,eff}}}{f_{\text{cd}}}} \tag{22}$$

where ε_{c0} is the peak strain of the concrete confined by the stirrups. The FRP reinforcement is supposed to be applied at both end of the columns for a length l_f (Fig. 8a). This arrangement is aimed at concentrating the confinement effect of retrofitting system in the portion of element where the major ductility is required.

The effect of FRP retrofitting is introduced into reinforced concrete elements by simply modifying the constitutive model of concrete fibers. For sake of simplicity, given that the confining effect exerted by the FRP wrapping is prevailing, the model considers only one single concrete constitutive law for the whole section.

Moreover, it is assumed that the effect of confinement is extended to the entire cross-section both for the cases of columns with and without steel jacketing reinforcement. Samples of the resulting stress–strain response in compression for a reference column cross-section fiber are reported in Fig. 8b considering different FRP layers.

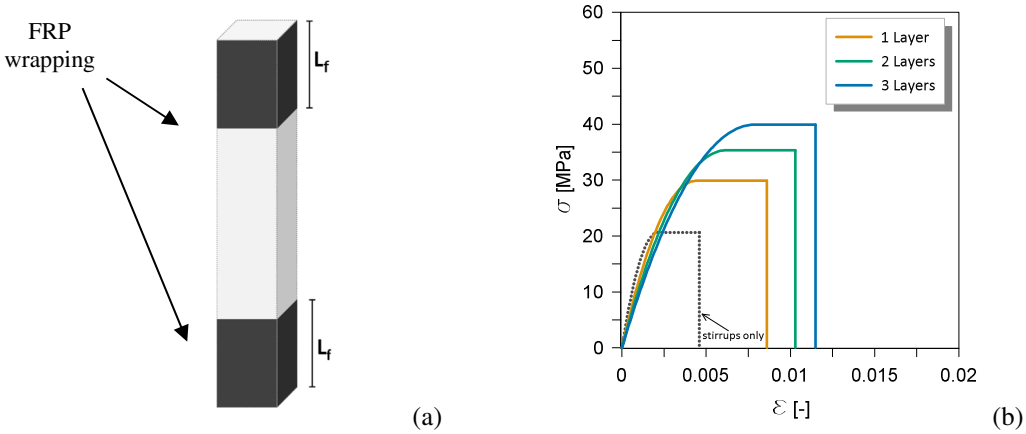

Figure 8: Details of FRP reinforcement of concrete elements: (a) Typical FRP arrangement for a column with generic confined height (l_a); (b) Samples of confined concrete stress–strain responses by varying the number of FRP layers.

3.2 Modelling of steel braces

Steel bracings are modelled using truss elements available in OpenSees. The steel is modelled adopting *Steel02* elastic-plastic with isotropic strain hardening (Giuffrè-Menegotto-Pinto material model). The model provides elastic linear behaviour and strain hardening defined by the yielding stress and strain (respectively f_{yb} and ε_{yb}), strain hardening factor (k), and ultimate strain (ε_{ub}). Steel elements are assumed to have a circular cross-section whose diameter is defined by the decision variable ϕ_{br}.

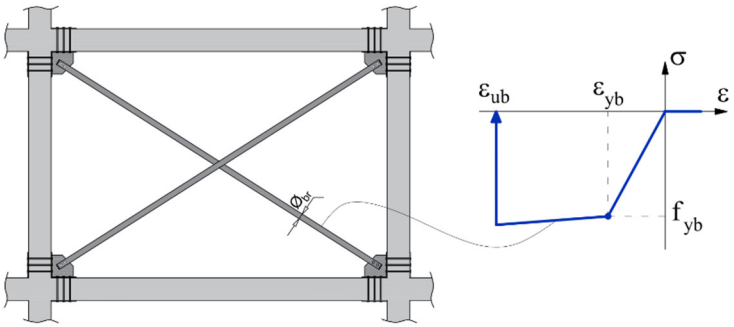

Figure 9: Typical arrangement of the concentric steel bracings.

Given that the constitutive law used provides strain hardening, so in order to limit the strain value of elements, *Steel02* is combined with *MinMax* material. The bracings elements are modeled using the OpenSees *trussSection* command. In Figure 9 the typical arrangement of bracing is reported together with the representation of the constitutive law of the material.

4 CASE-STUDY TEST OF THE OPTIMIZATION FRAMEWORK

4.1 Details of the reference structural and performance of the as-built structure

The effectiveness of the proposed framework is tested by performing the retrofitting optimization for a RC structure having structural configuration typical of buildings designed prior to the entry into force of seismic guidelines. In detail, the building consists of a five-storey reinforced concrete frames structure presenting uni-directional frames (Fig. 10). Reinforcement details of beams and columns are reported in Table 2.

RC members	***b*** (mm)	***h*** (mm)	**Longitudinal reinforcement**	**Transverse reinforcement**
Beams	800	300	4+4 Ø18	Ø6 / 200 mm
Columns	450	450	12 Ø18	Ø6 / 200 mm

Table 2: Geometrical dimensions and reinforcement details of RC elements.

Reinforced concrete elements are assumed to be made of poor resistance concrete having average unconfined strength f_{c0} = 20 MPa and steel rebars with nominal average yielding strength f_y = 455 MPa and strain hardening ratio is assumed equal to η = 0.01.

As regards seismic hazards, the building is supposed to be located in Cosenza (Italy), soil type C, the nominal life (V_N) is 100 years. The resulting return period is T_R=975 years. The structure has double symmetry in plan and it is regular in elevation. Vertical loads are modelled as point loads applied to the top node of each column as function of the respective tributary areas in plan. Rigid diaphragm behaviour is imposed at every floor.

The maximum interstory drift ratio, at which the DLLS condition is achieved, is set to $\delta_{i,max}$ = 0.005. Interstory drifts are monitored at each step of pushover analysis so that the damage limitation limit state is associated with top displacement of the structure which corresponds to the first exceeding of $\delta_{i,max}$.

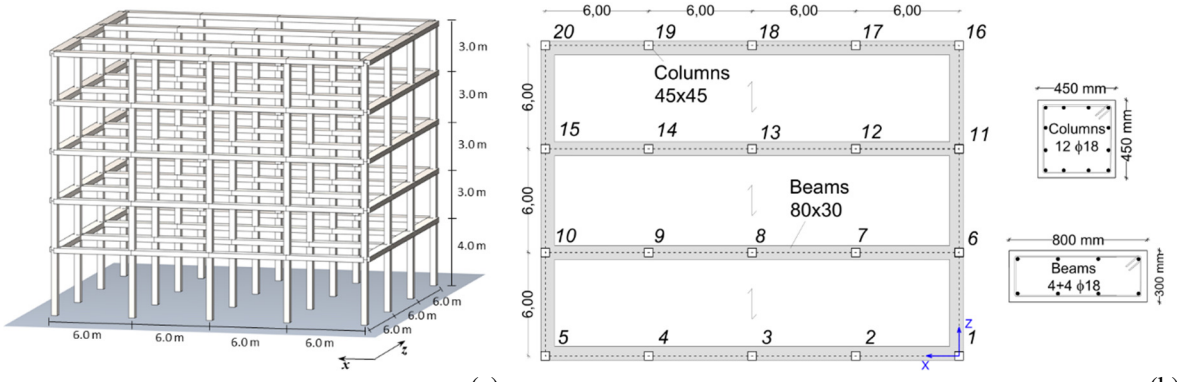

(a) (b)

Figure 10: Geometrical dimension of the reference structural model: (a) 3D frame view; (b) in plane dimensions.

A preliminary assessment of the as-built structure has been carried out to test its performance against the reference earthquake loads. For the sake of simplicity, pushover analysis is carried out by considering only a uniform profile for lateral loads acting along the z direction of the structure, which is supposed being the most vulnerable to seismic actions. As can be seen from Fig. 11, depicting the pushover curve in the ADRS plane together with and EAL curve compared to the one associated to code compliant building, the structure shows both reduced ductility and propension to be vulnerable against damage limit states.

$\zeta_{E,\mathrm{DLLS}}$	$\zeta_{E,\mathrm{LSLS}}$	λ_{DLLS}	λ_{LSLS}	EAL
0.906	0.812	0.0263	0.0027	1.381

Table 3: GA analysis parameters set up for the case study.

Results are also shown in the Table 3, showing the as-built configuration safety factors related to DLLS and LSLS smaller than unity ($\zeta_{E,\mathrm{DLLS}} = 0.9$ and $\zeta_{E,\mathrm{DLLS}} = 0.8$). This leads to a EAL value that is equal to 1.381. Seismic retrofitting interventions are therefore needed.

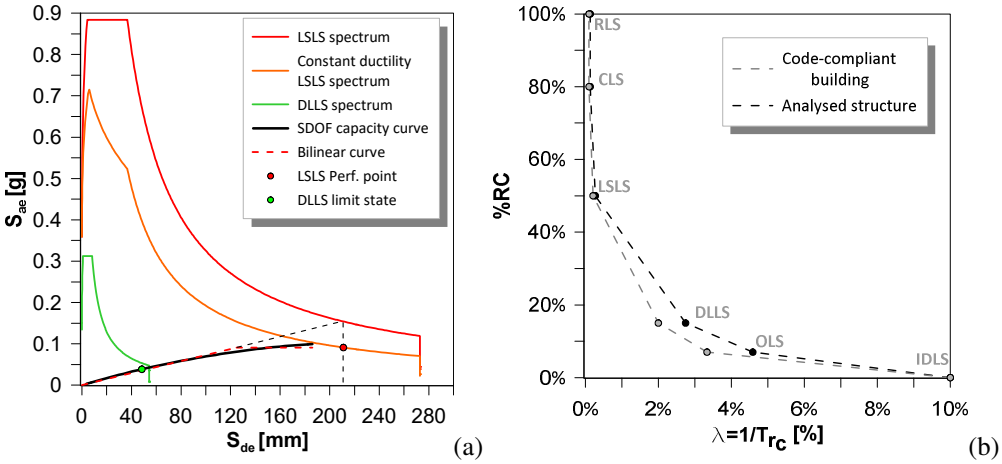

Figure 11: As-built preliminary test: (a) pushover curve in ADRS plane; (b) EAL curve compared with the curve related to code-compliant building.

4.2 Retrofitting system and hypotheses on the design space

The retrofitting system is composed of FRP wrapping of columns and concentric steel bracings. In order to reduce the computational effort of the analysis, the following restrictions are applied. Since the structure has a double symmetry in plane, the bracings are defined symmetrically on the two external transversal frames. In this way the n_{br} is the number of floors where the bracing systems are defined, starting from the ground floor, and $Ø_{br}$ is the diameter of the bracing, so that:

$$\begin{cases} n_{\mathrm{br}} \in & \left[0, n_{\mathrm{floor,max}}\right] \\ \phi_{\mathrm{br}} \in & \left[\phi_{\mathrm{min}}, \phi_{\mathrm{max}}\right] \end{cases} \tag{23}$$

where $n_{\mathrm{floor,max}}$ is the maximum number of floors of the structure to be potentially retrofitted (for the current case $n_{\mathrm{floor,max}} = 5$), $Ø_{\mathrm{min}}$ and $Ø_{\mathrm{max}}$ are the minimum and maximum bracing diameters allowed respectively.

The FRP sheets a have a thickness of $t_{f,1} = 0.337\ mm$ per layer, elastic modulus E_f = 230 GPa, ultimate stress referred to net area of the fibers $f_{fib,k}$ = 3250 MPa and ultimate strain ε_{fib}= 1,3%. For the implementation of FRP wrapping, it is assumed that a rounding of the column edges with a radius equal to $r_c = 25$ mm is carried out. The bracings are supposed to be made of S275 structural steel with $f_{yb} = 275$MPa , and elastic modulus $E_{\mathrm{sb}} = 210$ GPa .

To decrease the design space dimension, the analysis has been constrained to a limited number of columns for the confinement systems and to a restricted number of frames for the bracings. The following hypotheses are being placed:

i) The optimization space for retrofitted columns by FRP jacketing is limited to the first two floors (red area Fig. 12).
ii) The maximum number of FRP layers is 4.
iii) The design space for the bracings is restricted to the central transversal frames (blue area Fig. 12).
iv) Bracing diameter range of optimization is 20-100 mm and it vary with a minimum step size $\Delta Ø_{br}$ of 10 mm.

The resulting size of the design space is then of 6 integers that encode the number of floors where the bracings are defined (n_{br}), 9 discrete natural variables for the bracings diameter ($Ø_{br}$), 4 naturals encoding the number of FRP layers (n_{FRP}), and 40 Boolean variables for the FRP position ($\mathbf{p}$). Therefore, the research space consists of 2×10^{14} different solutions.

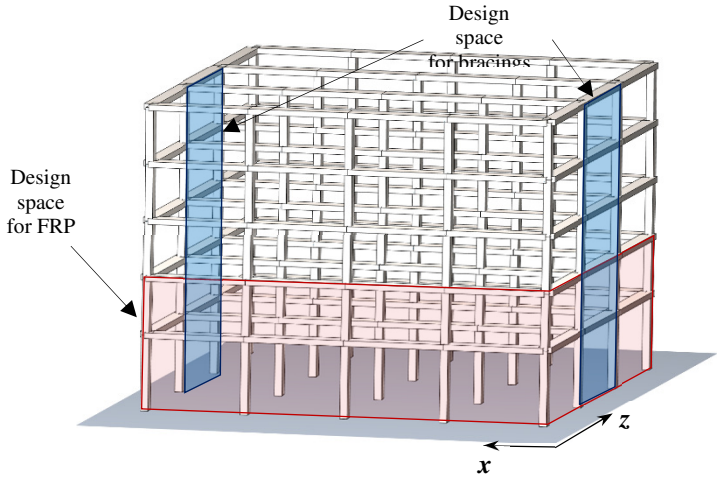

Figure 12: Design space representation on the case study structure.

4.3 Optimization results

The analysis was carried out starting from a first generation of 100 randomly generated. Individuals. The algorithm proceeds by creating 100 new child every generation selecting the parents from a tournament selection on three randomly selected parents. In the following Table 4 a summary of the GA framework parameter settings is reported.

Generation dimension	Number of off-spring	Tournament size **k**	Max generations	Max stall
100	100	3	20	5

Table 4: GA analysis parameters set up for the case study.

The convergence history of the optimization is also shown in Fig. 13, where the optimal solution is found in correspondence of the eighteenth generation with a stagnation equal to two. As shown in the convergence Fig. 13a, the proper definition of the genetic operators allows a gradual transition between the exploration and exploitation phases.

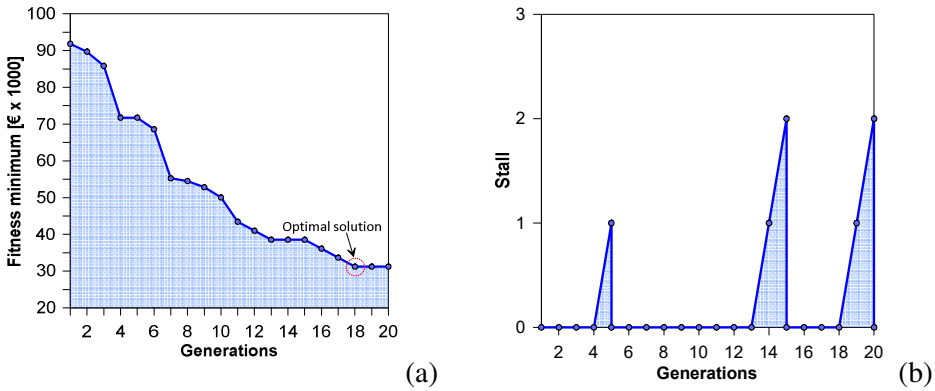

Figure 13: GA analysis performance results: (a) Convergence history; (b) Progressive optimal results stall.

The optimal solution obtained is represented in Fig. 14. It can be observed that the latter is characterized by only steel bracing retrofitting on the external frames for the first two floors, while no specific FRP interventions were required except from local reinforcement of braced frame columns. The optimal configuration bracings had a diameter $Ø_{br}$ = 50 mm, which is equivalent to a cross-section area of $A_{br} = 19.6\,\text{cm}^2$. The overall cost of this intervention was 31299€.

Bracings were basically introduced to reduce lateral deformability of the frames, especially in along z direction, and prevent DLLS. However, bracings also provide additional strength and deformation capacity, so their contribution is also reflected on the LSLS. This double effect, combined with the overall lower cost of bracings with respect to FRP wrapping, has led the algorithm to individuate only steel bracings (as in Fig. 14) as the minimum cost solution.

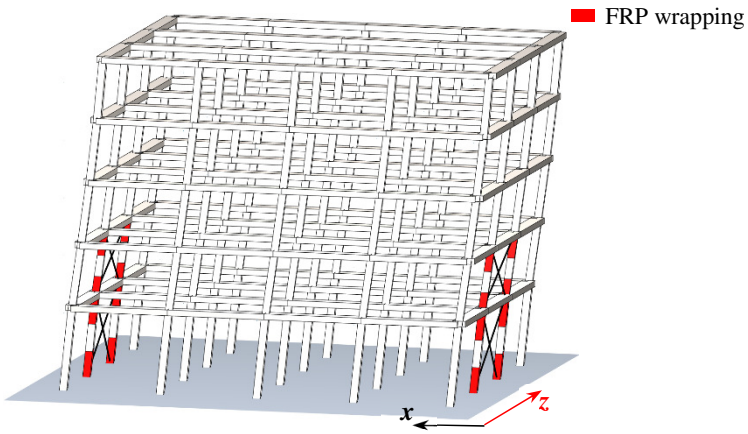

Figure 14: Retrofitting configuration of the optimal solution (deformed shape).

The performance of the optimal solution is shown in Figure 15 in terms of pushover and EAL curves. The increase in stiffness due to the retrofitting system leaded to a reduced displacement demand, which combined with the additional resistance and ductility provided by the steel bracing allowed satisfying both LS and DL limit states. As reported in Table 5, safety factor related to damage limit state is barely close to the unity ($\zeta_{E,DLLS} = 1.025$) whereas the safety factor related to LSLS is $\zeta_{E,LSLS} = 1.585$.

The EAL curve displayed in Fig. 15b shows a noteworthy reduction with respect to as-built configuration EAL, resulting in EAL = 1.01%. Given that the objective function does not directly consider the value of the EAL associated with each tentative solution (only the cost is minimized), the optimal configuration does not lead to EAL value that is optimized with respect

to the code compliant building. However, the proposed framework improves the quality of the retrofitting design by providing a cost-optimized intervention with a control on the EAL.

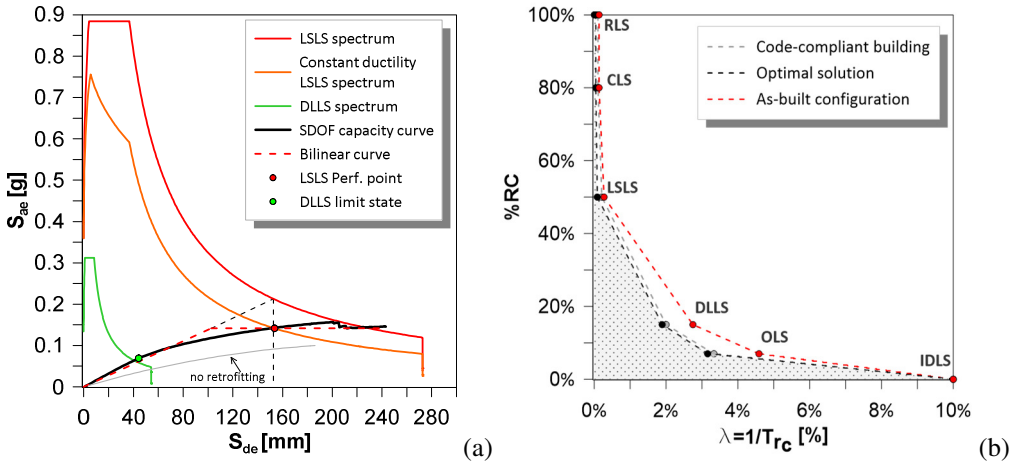

Figure 14: Optimal solution: (a) pushover curve in ADRS plane; (b) EAL curve.

n_{FRP}	n_{br}	$Ø_{br}$ (mm)	$\zeta_{E,DLLS}$	$\zeta_{E,LSLS}$	**EAL** *(%RC)*	**Cost (€)**
1	2	50	1.025	1.585	1.009	31229

Table 5: Optimization analysis results

5 CONCLUSIONS

The paper has presented a novel optimization framework aims to minimize costs related to retrofitting intervention on RC frame structures. The framework is based on genetic algorithm developed in MatLab® which interfaces with a 3D fiber-section model realized in OpenSEES. Two different typology of retrofitting system are considered: FRP jacketing of columns and steel bracings.

The main target of the algorithm is to seek the retrofitting configuration that optimize the intervention costs taking into account in indirect way of the expected annual loss value referring to that requested by the reference technical code. The performance of each tentative solution is evaluated starting from the results of non-linear static analysis in the framework of N2 method. Through a case study implementation, it has been shown that the proposed framework can pin-point optimal retrofitting arrangement in efficient way. Eventually, the results obtained have been compared with the outcomes of an optimization procedure that neglect the EAL assessment.

An extensively usage of the framework will allow improving the management of the funds allocated to seismic retrofitting of existing structures enhancing the overall structural safety of building heritage.

REFERENCES

[1] C. Chisari, C. Bedon, Multi-Objective Optimization of FRP Jackets for Improving the Seismic Response of Reinforced Concrete Frames. *American Journal of Engineering and Applied Sciences*, **9(3)**, 669-79, 2016.

[2] H. Seo, J. Kim, M. Kwon, Optimal seismic retrofitted RC column distribution for an existing school building. *Engineering Structures*, **168**, 399-404, 2018.

[3] N. Pollini, O. Lavan, O. Amir, Minimum-cost optimization of nonlinear fluid viscous dampers and their supporting members for seismic retrofitting. *Earthquake Engineering & Structural Dynamics*, **46**, 1941–61, 2017.

[4] F. Braga, R. Gigliotti, R. Laguardia, Intervention cost optimization of bracing systems with multiperformance criteria. *Engineering Structures*, **182**, 185-197, 2019.

[5] O. Lavan, G.F. Dargush, Multi-objective evolutionary seismic design with passive energy dissipation systems. *Journal of Earthquake Engineering*, **13(6)**, 758-90, 2009.

[6] R. Falcone, F. Carrabs, R. Cerulli, C. Lima, E. Martinelli, Seismic retrofitting of existing rc buildings: a rational selection procedure based on genetic algorithms. *Structures*, **22**, 310–326, 2019.

[7] G.S. Papavasileiou, D.C. Charmpis, N.D. Lagaros, Optimized seismic retrofit of steel-concrete composite buildings. *Engineering Structures*, **213**, 110573, 2020.

[8] F. Di Trapani, M. Malavisi, G.C. Marano, A.P. Sberna, R. Greco, Optimal seismic retrofitting of reinforced concrete buildings by steel-jacketing using a genetic algorithm-based framework. *Engineering Structures*, **219**, 110864, 2020.

[9] G.M. Calvi, Choices and criteria for seismic strengthening. *Journal of Earthquake Engineering*, **17(6)**, 769-802, 2013.

[10] F. McKenna, G.L. Fenves, M.H. Scott, *Open system for earthquake engineering simulation*. University of California Berkley, 2000.

[11] E. Cosenza, C. Del Vecchio, M. Di Ludovico, M. Dolce, C. Moroni, A. Prota, E. Renzi, The Italian guidelines for seismic risk classification of constructions: technical principles and validation. *Bulletin of Earthquake Engineering*, **16**, 5905–5935, 2018.

[12] P. Fajfar, A Nonlinear Analysis Method for Performance-Based Seismic Design. *Earthquake Spectra*, **16(3)**, 573-92, 2000.

[13] *Norme tecniche per le costruzioni. Decreto ministeriale 17 gennaio 2018*, Ministero delle infrastrutture e dei trasporti, 2018.

[14] *Eurocode 8. Design of structures for earthquake resistance - Part 3: Assessment and retrofitting of buildings*, European Committee for Standardization, 2005.